

Linking boundary conditions for kinetic and hydrodynamic description of fermion gas

O. E. Raichev *Institute of Semiconductor Physics NAS of Ukraine, Prospekt Nauki 41, 03028 Kyiv, Ukraine*

(Received 20 September 2021; revised 11 January 2022; accepted 14 January 2022; published 28 January 2022)

An approximate analytical solution of the boundary slip problem in magnetic field is obtained by using the general form of boundary conditions for the distribution function of fermions with the isotropic energy spectrum. Exact numerical calculations of the slip length for different models of angle-dependent specularly parameter and application of the results to the description of the Poiseuille flow demonstrate the reliability of the approximate solution for establishing a direct link between the hydrodynamic and the kinetic approaches to transport in bounded fermion systems.

DOI: [10.1103/PhysRevB.105.L041301](https://doi.org/10.1103/PhysRevB.105.L041301)

Studies of hydrodynamic phenomena in electron transport in solids [1–29] are most often based on investigation of current flow in the samples of small size where the presence of boundaries considerably influences the transport properties. In particular, the nonideal boundaries where electrons change their momenta as a result of nonspecular reflection are responsible for drift velocity gradients affecting the hydrodynamic flow via the viscosity. The hydrodynamic regime occurs when the rate of electron-electron collisions conserving the local momentum of electron system becomes larger than the rates of momentum-changing scattering of electrons by impurities, phonons, and boundaries. In this case, the transport is described in terms of the coordinate-dependent drift velocity $\mathbf{u}(\mathbf{r})$, or the related electric current $\mathbf{j} = en\mathbf{u}$, where e and n are the electron charge and density, governed by the Navier-Stokes equation (NSE). Beyond the hydrodynamic regime, one has to use a more general albeit more complicated approach based on solution of the Boltzmann kinetic equation for the distribution function $f_{\mathbf{p}}(\mathbf{r})$ that depends on both the momentum \mathbf{p} and the coordinate \mathbf{r} . The kinetic equation approach covers all classical transport regimes and is indispensable for the description of the transition between the quasiballistic and the hydrodynamic regimes, when the modifications of electrical resistance dependence on the temperature and magnetic field serve as hallmarks for the onset of hydrodynamic behavior [13,24,26–29].

Establishing a connection between the Boltzmann equation and the NSE in bounded systems is of particular importance. The NSE itself can be derived from the Boltzmann equation either by applying the method of moments [30] or, equivalently, by expanding $f_{\mathbf{p}}(\mathbf{r})$ into series of harmonics of the angle of \mathbf{p} , and neglecting the higher-order moments under the restrictions imposed by the hydrodynamic regime. This commonly accepted procedure is straightforward because the relation between the current and the distribution function is direct and assumes just an integration over the entire momentum space. However, a connection between the boundary conditions (BCs) used in the kinetic theory and the hydrodynamic BC is not so obvious because of the

different mathematical natures of these conditions. The hydrodynamic BC relates the tangential component of \mathbf{u} with its derivative at the boundary. The kinetic BC relates the distribution functions from *different* momentum semispaces corresponding to incident and reflected particles. Furthermore, the boundary reflection mixes different angular harmonics of $f_{\mathbf{p}}(\mathbf{r})$, so the use of truncated sets of moments generally fails near the boundary.

The general form of the hydrodynamic BC for both three- (3D) and two-dimensional (2D) systems is

$$\mathbf{u}_t = l_S \nabla_n \mathbf{u}_t, \quad (1)$$

where \mathbf{u}_t is the tangential component of the drift velocity, $\nabla_n \mathbf{u}_t$ is its normal inward derivative, and l_S is the slip length that plays an important role in hydrodynamics. The boundary slip problem, i.e., determination of the relation of l_S to the kinetic properties of gas or liquid became a subject of study since the foundation of the kinetic theory [31]. For 3D gases, approximate results relating l_S to the viscosity have been obtained, and the exact values of l_S have been calculated in the limit of fully diffuse boundary reflection [32]. The increase in l_S with increasing degree of specularly has been also discussed [14,31–33]. Until recently, the existing results in the boundary slip problem were ignored in the rapidly developing hydrodynamics of fermion gas in solids, and l_S was often considered as a freely adjustable parameter. The authors of Ref. [34] have drawn attention to the problem and calculated l_S for 2D fermions in the cases of fully diffuse and nearly specular reflections. Despite these achievements, a full and clear correspondence between the kinetic and the hydrodynamic BCs is still missing.

In this Letter, an approximate expression for the slip length is derived by using the general form of BC for the distribution function and in the presence of a magnetic field. Next, the exact slip length is calculated for nonzero specularly of boundary reflection, including different models of angle-dependent specularly parameter. It is found that the exact results approach the approximate ones when specularly increases. This important property gives more reliability to

the approximate results and justifies their application in the hydrodynamics of fermion systems as further demonstrated by comparing hydrodynamic and kinetic solutions of the transport problem in narrow 2D channels.

First, a brief review of the BC used in the kinetic theory is presented. It is assumed below that the particles are described by the isotropic energy spectrum $\varepsilon = \varepsilon_p$ and the boundary scattering is elastic, $|\mathbf{p}| = |\mathbf{p}'| = p_\varepsilon$. The BC for the distribution function at the hard-wall boundary in 3D media is

$$f_{\mathbf{p}}^+ = f_{\mathbf{p}}^- + \int_+ \frac{d\Omega'}{4\pi} c'_n P_\varepsilon(\mathbf{p}, \mathbf{p}') (f_{\mathbf{p}'}^- - f_{\mathbf{p}}^-), \quad (2)$$

where $f_{\mathbf{p}}^\pm = f_{\mathbf{p}_t, \pm p_n}$ are the distribution functions of reflected (+) and incident (-) particles, $p_n = p_\varepsilon \sin \varphi$ and \mathbf{p}_t are the normal and tangential components of the momentum, $\mathbf{c} = \mathbf{p}/|\mathbf{p}|$ is the unit vector along the momentum, and $\int_+ \frac{d\Omega'}{4\pi} \dots$ denotes averaging over the solid angle of \mathbf{p}' in the + hemisphere, where $\sin \varphi' > 0$. Equation (2) is a general form of the integral relation between the distribution functions of incident and reflected particles guaranteeing zero particle flow through the boundary for arbitrary $f_{\mathbf{p}}$. This equation can be derived from the quantum-mechanical reflection problem, see Refs. [35–37], and Sec. 44 in Ref. [38]. The boundary scattering is described by the function P_ε , which is symmetric with respect to permutation of momenta, $P_\varepsilon(\mathbf{p}, \mathbf{p}') = P_\varepsilon(\mathbf{p}', \mathbf{p})$ and equal to zero at $\varphi = 0$ as the reflection is specular at grazing incidence. For the macroscopically isotropic boundary, $P_\varepsilon(\mathbf{p}, \mathbf{p}')$ is invariant with respect to simultaneous rotation of \mathbf{p}_t and \mathbf{p}'_t . The probability of specular reflection at angle φ is given by the specular parameter $r_{\varepsilon\varphi} = 1 - \int_+ \frac{d\Omega'}{4\pi} c'_n P_\varepsilon(\mathbf{p}, \mathbf{p}')$. In the case of noncorrelated boundary scattering, when the nonspecular reflection (whose probability is $1 - r_{\varepsilon\varphi}$) is isotropic, Eq. (2) is simplified to the form

$$f_{\mathbf{p}}^+ = r_{\varepsilon\varphi} f_{\mathbf{p}}^- + (1 - r_{\varepsilon\varphi}) \bar{f}_\varepsilon, \quad \bar{f}_\varepsilon = \int_+ \frac{d\Omega}{4\pi} c_n (1 - r_{\varepsilon\varphi}) f_{\mathbf{p}}^- / \int_+ \frac{d\Omega}{4\pi} c_n (1 - r_{\varepsilon\varphi}). \quad (3)$$

The limiting cases $r_{\varepsilon\varphi} = 1$ and $r_{\varepsilon\varphi} = 0$ describe fully specular and fully diffuse reflection. Despite less generality compared to Eq. (2), Eq. (3) is far more convenient for applications because it is not an integral relation, and the boundary properties can be modeled by specifying the magnitude and the angular dependence of $r_{\varepsilon\varphi}$.

The current-penetrable boundary can be described by the in-flow BC [39]: $f_{\mathbf{p}}^+ = \mathcal{G}_\varepsilon(\varphi)$, where \mathcal{G} models inward emission of particles. This BC can be viewed as a particular case of Eq. (3) in the fully diffuse limit.

Equations (2) and (3) are adopted for 2D systems by reducing \mathbf{p}_t to the scalar variable $p_\varepsilon \cos \varphi$ and by substituting $\int_+ \frac{d\Omega'}{4\pi} \dots \rightarrow \int_0^\pi \frac{d\varphi'}{2\pi} \dots$. The function $P_\varepsilon(\mathbf{p}, \mathbf{p}')$ can be written as $P_\varepsilon(\varphi, \varphi')$.

Consider now a steady-state linear-transport classical kinetic problem for charged fermions in a homogeneous magnetic-field \mathbf{B} directed parallel to the boundary. The distribution function is presented as

$$f_{\mathbf{p}}(\mathbf{r}) = f_\varepsilon + \delta f_{\mathbf{p}}(\mathbf{r}) = f_\varepsilon - \frac{\partial f_\varepsilon}{\partial \varepsilon} [g_{\mathbf{p}}(\mathbf{r}) - e\Phi(\mathbf{r})], \quad (4)$$

where f_ε is the equilibrium Fermi-Dirac distribution and $\Phi(\mathbf{r})$ is the electrostatic potential. The BCs given by Eqs. (2) and (3) are valid as well for the nonequilibrium correction $g_{\mathbf{p}}$. In the hydrodynamic regime,

$$g_{\mathbf{p}} = g_0 + \mathbf{g}_\varepsilon \cdot \mathbf{c} + Q_\varepsilon^{\alpha\beta} (c_\alpha c_\beta - \delta_{\alpha\beta}/d), \quad (5)$$

where d is the dimensionality of the system, $g_0(\mathbf{r}) = eV(\mathbf{r})$, V is the nonequilibrium electrochemical potential, $\mathbf{g}_\varepsilon(\mathbf{r})$ describes the drift velocity $\mathbf{u} = \langle \mathbf{g}_\varepsilon/p_\varepsilon \rangle$, and $Q_\varepsilon^{\alpha\beta}(\mathbf{r})$ is the symmetric tensor describing the momentum flow density $\Pi_{\alpha\beta} = 2n \langle Q_\varepsilon^{\alpha\beta} \rangle / (d+2)$. The average over energy is $\langle A_\varepsilon \rangle \equiv \int d\varepsilon D_\varepsilon v_\varepsilon p_\varepsilon (-\partial f_\varepsilon / \partial \varepsilon) A_\varepsilon / dn$, where D_ε is the density of states and v_ε is the absolute value of the group velocity. Equation (5) is a truncated expansion of the exact $g_{\mathbf{p}}$ in powers of c_α . Beyond the hydrodynamic regime, it is necessary to include all higher-order terms in this expansion.

It is specified below that a flat boundary is placed at $y = 0$ and the magnetic field is directed along the Oz axis. Evaluating the collision integral in the kinetic equation in the elastic relaxation-time approximation, and taking into account that the drift velocity depends only on y , one can express the components of $Q_\varepsilon^{\alpha\beta}$ (and, hence, of the viscous stress tensor $-\Pi_{\alpha\beta}$) as follows:

$$Q_\varepsilon^{xx} = -Q_\varepsilon^{yy} = l_\perp \omega_c \tau \nabla_y g^x, \quad Q_\varepsilon^{xy} = -\frac{l_\perp}{2} \nabla_y g^x, \\ Q_\varepsilon^{xz} = \frac{l_\parallel}{2} \omega_c \tau \nabla_y g^z, \quad Q_\varepsilon^{yz} = -\frac{l_\parallel}{2} \nabla_y g^z, \quad Q_\varepsilon^{zz} = 0, \quad (6)$$

where $\omega_c = -eB/mc$ is the cyclotron frequency and $m = p_\varepsilon/v_\varepsilon$ is the effective mass. The lengths $l_\perp = l_\varepsilon/[1 + (2\omega_c\tau)^2]$ and $l_\parallel = l_\varepsilon/[1 + (\omega_c\tau)^2]$, characterize the stress for the drift in the directions transverse and longitudinal with respect to \mathbf{B} . The stress at $B = 0$ is determined by $l_\varepsilon = v_\varepsilon\tau$, where $1/\tau = 1/\tau_2 + 1/\tau_e$ [9] is the relaxation rate of the second angular harmonic of the distribution function. This rate is a sum of the contributions from the momentum-changing scattering and from the momentum-conserving scattering between the particles, characterized by the times τ_2 and τ_e , respectively. In the hydrodynamic regime, $\tau_2 \gg \tau_e$, so $l_\varepsilon \simeq l_e = v_\varepsilon\tau_e$. Applying Eqs. (5) and (6) together with the hydrodynamic expression $\mathbf{g}_\varepsilon(\mathbf{r}) = p_\varepsilon \mathbf{u}(\mathbf{r})$ into the kinetic equation, multiplying the latter by \mathbf{p} , and integrating over momentum, one gets the linearized NSE,

$$n^{-1} \eta_{\alpha\beta} \nabla_y^2 u_\beta + (eB/c) \epsilon_{z\alpha\beta} u_\beta - \zeta u_\alpha = e \nabla_\alpha V, \quad (7)$$

which is valid both for 3D media and for 2D layers in the xy plane. Here, $\epsilon_{z\alpha\beta}$ is the antisymmetric unit tensor, $\zeta = (m/\tau_1)$, τ_1 is the relaxation time of the first angular harmonic of the distribution function, also known as the transport time, and $\eta_{\alpha\beta}$ is the dynamic viscosity tensor. The components of $\eta_{\alpha\beta}$ contributing to Eq. (7) are transverse, longitudinal, and Hall viscosities,

$$\eta_{xx} = n \frac{\langle p_\varepsilon l_\perp \rangle}{d+2}, \quad \eta_{zz} = n \frac{\langle p_\varepsilon l_\parallel \rangle}{d+2}, \quad \eta_{yx} = 2n \frac{\langle \omega_c \tau p_\varepsilon l_\perp \rangle}{d+2}. \quad (8)$$

The BC for \mathbf{u} in Eq. (7) can be derived on an equal footing by using Eqs. (5) and (6). After expressing $g_{\mathbf{p}}$ in terms of $g_{\mathbf{p}}^\pm = g_{\mathbf{p}_t, \pm p_n}$, the tangential momentum flow density in the direction

normal to the boundary is

$$\Pi_{\alpha y}(\mathbf{r}) = nd \left\langle \int_+ \frac{d\Omega}{4\pi} c_\alpha c_y [g_{\mathbf{p}}^+(\mathbf{r}) - g_{\mathbf{p}}^-(\mathbf{r})] \right\rangle, \quad (9)$$

where $\alpha = x, z$ for 3D and $\alpha = x$ for 2D systems. Far from the boundary, Eq. (9) is an identity since it is reduced to the definition of $\Pi_{\alpha y}$ as the integral of the product $p_\varepsilon v_\varepsilon c_\alpha c_y f_{\mathbf{p}}$ over the momentum space. Further application of Eq. (9) at the boundary $y = 0$ is based on Maxwell's idea [31]. It is assumed that the hydrodynamic form (5), which is valid away from the boundary, remains valid everywhere for the *incident* (−) particles. Expressing $g_{\mathbf{p}}^+$ in Eq. (9) through $g_{\mathbf{p}}^-$ with the aid of the BC (3) and then using Eq. (5) for $g_{\mathbf{p}}^-$, one finally obtains two terms proportional to $\langle g_\varepsilon^\alpha \rangle$ and $\langle Q_\varepsilon^{\alpha y} \rangle$. After applying Eq. (6) together with $\mathbf{g} = p_\varepsilon \mathbf{u}$, Eq. (9) assumes the form of Eq. (1), where l_S is expressed as

$$l_S^{(i)} = \frac{\langle p_\varepsilon l_i \lambda_2^+ \rangle}{\langle p_\varepsilon \lambda_1^- \rangle}, \quad \lambda_k^\pm = \int_0^{\pi/2} d\varphi (1 \pm r_{\varepsilon\varphi}) \cos^d \varphi \sin^k \varphi, \quad (10)$$

where $i = \perp, \parallel$ for $d = 3$ and $i = \perp$ for $d = 2$. Application of the general BC (2) instead of BC (3) is reduced to the formal substitution $r_{\varepsilon\varphi} \rightarrow \tilde{r}_{\varepsilon\varphi}$ in Eq. (10), where

$$\tilde{r}_{\varepsilon\varphi} = 1 - \int_+ \frac{d\Omega'}{4\pi} \sin \varphi' P_\varepsilon(\mathbf{p}, \mathbf{p}') \left[1 - \frac{\cos \varphi'}{\cos \varphi} \cos \theta_- \right], \quad (11)$$

and θ_- is the difference of the azimuthal angles of \mathbf{p} and \mathbf{p}' . In the 2D case $\tilde{r}_{\varepsilon\varphi} = 1 - \int_0^\pi \frac{d\varphi'}{2\pi} \sin \varphi' P_\varepsilon(\varphi, \varphi') [1 - \cos \varphi' / \cos \varphi]$.

If energy dependence of $r_{\varepsilon\varphi}$ is absent or inessential, Eq. (10) is rewritten as

$$l_S^{(i)} = \Lambda_d \ell_i, \quad \ell_i = (d+2)\eta_i / \langle p_\varepsilon \rangle n, \quad \Lambda_d = \lambda_2^+ / \lambda_1^-, \quad (12)$$

where $\eta_\perp \equiv \eta_{xx}$ and $\eta_\parallel \equiv \eta_{zz}$, see Eq. (8). The slip length is equal to the product of the slip coefficient Λ_d by the length ℓ_i related to the diagonal components of the viscosity. The relation of l_S to viscosity, known previously at $B = 0$, persists at finite B , when the viscosity is B dependent. Equation (12) is applicable, e.g., if the specularity parameter is a constant r . Then the slip coefficients are $\Lambda_3 = (8/15)(1+r)/(1-r)$ [33] and $\Lambda_2 = (3\pi/16)(1+r)/(1-r)$. Next, Eq. (12) is always applicable to degenerate fermion gases as the energy average fixes ε at the Fermi level ε_F . Equations (10)–(12) are derived in the hydrodynamic regime $l \ll l_1$, where $l = \langle l_\varepsilon \rangle$ and $l_1 = \langle v_\varepsilon \tau_1 \rangle$ is the transport mean free path length. They apply for fermions with an arbitrary energy spectrum and for ordinary gases if f_ε is the Boltzmann distribution.

The subsequent consideration contains a more detailed calculation of l_S and applications of the results to a transport problem. The case of degenerate fermion gas is studied, so $\ell_i = l_i$ at $B \neq 0$ and $\ell_i = l$ at $B = 0$. Since $\varepsilon = \varepsilon_F$, the energy index is omitted ($l_\varepsilon = l$, $v_\varepsilon = v$, etc.) here and below.

The results given by Eqs. (10)–(12) are approximate because the distribution function of incident particles loses its hydrodynamic form in the narrow Knudsen layer near the boundary [32]. To improve the accuracy and to find the exact slip length, both numerical and analytical methods have been

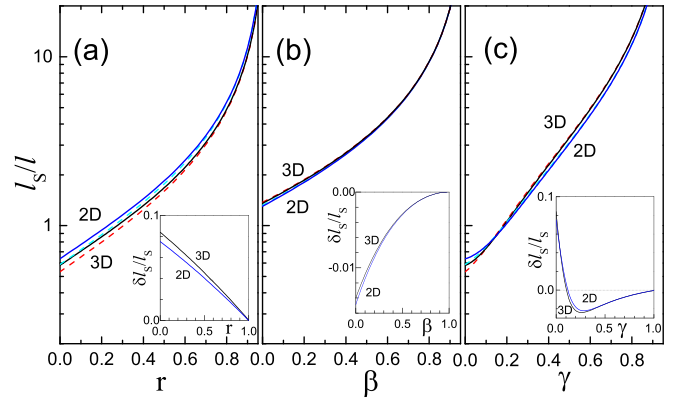


FIG. 1. Exact (solid) and approximate (dashed) slip lengths for different specularity parameters: (a) $r_\varphi = r$, (b) $r_\varphi = 1 - (1 - \beta) \sin \varphi$, and (c) $r_\varphi = \exp[-(\gamma^{-1} - 1) \sin^2 \varphi]$. The insets show the relative deviation of the exact results from the approximate ones.

developed for 3D gases [33,40–45]. The problem of *exact* slip length is reduced to solution of an integral equation for the drift velocity near the boundary. Below, this problem is solved at $B = 0$, by exploiting the integral equation for the current density $\mathbf{j} = en\mathbf{u}$ in a 2D channel obtained [2] from the Boltzmann equation with application of the BC (3), see also Ref. [28]. This equation is easily generalized for 3D fermions and adopted to the case of a single boundary at $y = 0$. It is convenient to present the tangential component of \mathbf{u} as $u_\alpha(y) = u_h(y) + \delta u(y)$ where hydrodynamic part u_h obeys Eq. (7) at $y \gg l$ and δu is a near-boundary correction. In the hydrodynamic regime, u_h varies on the diffusion length $\sqrt{l l_1 / (d+2)}$ which is much larger than l . Thus, near the boundary one can apply the linear form $u_h(y) = h + h'y$ and reduce the integral equation for $u_\alpha(y)$ to the following one:

$$\delta u(y) - \int_0^\infty \frac{dy'}{l} \mathcal{K}(y, y') \delta u(y') = lh'F_1^+(y) - hF_0^-(y), \quad (13)$$

where

$$\mathcal{K}(y, y') = a_d \int_0^{\pi/2} d\varphi \frac{\cos^d \varphi}{\sin \varphi} \left[e^{-|y-y'|/l \sin \varphi} + r_\varphi e^{-(y+y')/l \sin \varphi} \right], \quad (14)$$

$$F_k^\pm(y) = a_d \int_0^{\pi/2} d\varphi \cos^d \varphi \sin^k \varphi (1 \pm r_\varphi) e^{-y/l \sin \varphi}, \quad (15)$$

with $a_3 = 3/4$ and $a_2 = 2/\pi$. The approximate slip length given by Eq. (12) is found by integrating both sides of Eq. (13) over y from 0 to ∞ and neglecting the integral term in the resulting equation. Indeed, in this way one obtains $l_S = lF_2^+(0)/F_1^-(0)$, which is identical to Eq. (12) at $B = 0$ since $F_k^\pm(0) = a_d \lambda_k^\pm$. The exact slip length $l_S = h/h'$ is determined from the requirement that the solution $\delta u(y)$ of Eq. (13) goes to zero at $y \gg l$. The difference δl_S between the exact and the approximate slip lengths is $\delta l_S = -\int_0^\infty dy F_0^-(y) \delta u(y) / lh'F_1^-(0)$. Whereas δl_S can be either positive or negative, the relative deviation $\delta l_S/l_S$ is always numerically small.

A comparison of the exact and approximate l_S calculated within several models of r_φ is shown in Fig. 1 for both 3D

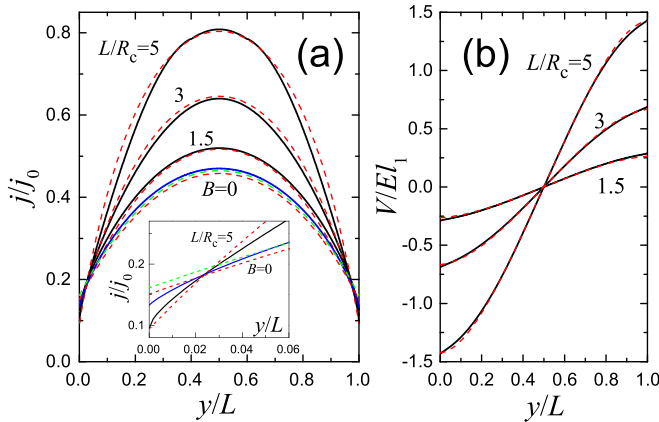


FIG. 2. Kinetic (bold lines) and hydrodynamic (dashed red lines) distributions of the tangential current density (a) $j(y)$ and (b) Hall potential $V(y)$ across the 2D channel with equal fully diffuse boundaries at $l_1/L = 5$ and $l_1/l_e = 25$ for several values of B defined by the ratio of channel width to cyclotron radius: $L/R_c = 0, 1.5, 3$, and 5 . The dashed green line is the distribution at $B = 0$ obtained with the exact slip length $0.637l$. The current and the potential are given in units of $j_0 = \sigma_0 E$ and El_1 , where E is the driving electric field along the channel and $\sigma_0 = e^2 n \tau_1 / m$ is the Drude conductivity. The inset shows the region near $y = 0$.

and 2D systems. The model of angle-independent $r_\varphi = r$ with $r \in [0, 1]$ is often applied in transport problems, although the absence of angular dependence of the reflection probability is a rough assumption, especially near $\varphi = 0$ and $\varphi = \pi$. The model $r_\varphi = 1 - (1 - \beta) \sin \varphi$ with $\beta \in [0, 1]$ reflects the property $P_\varepsilon(\mathbf{p}, \mathbf{p}') \propto p_n p'_n$ following from the treatment of boundary scattering in the Born approximation [36]. This model, however, does not describe fully diffuse boundaries. The model $r_\varphi = \exp[-(\gamma^{-1} - 1) \sin^2 \varphi]$ with $\gamma \in [0, 1]$ is free from this disadvantage.

The slip length is the smallest for fully diffuse reflection, when the calculations give $l_S/l = 0.582$ for 3D, in agreement with [43,44], and $l_S/l = 0.637$ for 2D fermions. The absolute value of the relative deviation $\delta l_S/l_S$ is the largest in this case (however, less than 9%), and decreases with increasing specularity. For angle-independent model, the exact l_S does not simply scale as $(1+r)/(1-r)$ with respect to its value at $r = 0$ but approaches the approximate value given by Eq. (12). For $r_\varphi = 1 - (1 - \beta) \sin \varphi$, both $|\delta l_S|/l_S$ and the difference between 2D and 3D cases are very small. The model $r_\varphi = \exp[-(\gamma^{-1} - 1) \sin^2 \varphi]$ shows sign inversion of δl_S : the approximate value of l_S , which is the lower bound of the exact solution for low specularity, becomes the upper bound for higher specularity at $\gamma \simeq 0.12$.

The smallness of $\delta l_S/l_S$ justifies application of Eq. (12) in the hydrodynamic BC (1). This conclusion has been tested by calculating the distributions of current density $j(y)$ and electrochemical potential $V(y)$ in a narrow 2D channel of width L . The results obtained from a numerical solution of the kinetic equation with the BC (3) [28] have been compared to the approximate analytical results obtained from Eq. (7) with the BC given by Eqs. (1) and (12), under the conditions of hydrodynamic regime, $l_e/l_1 \ll 1$ and $l_e/L \ll 1$. Several representative plots are shown in Figs. 2 and 3. If l_e is estimated

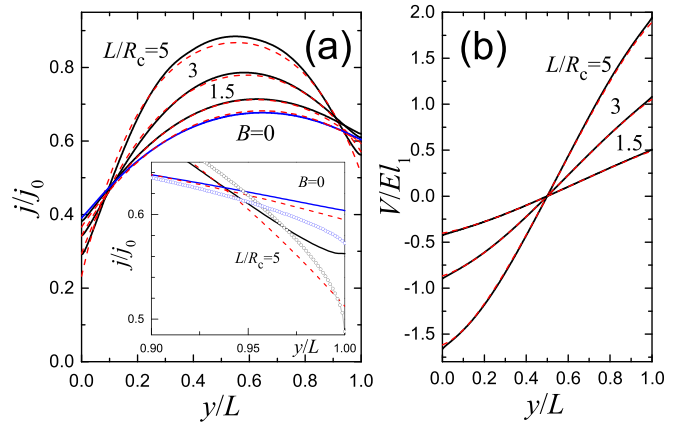


FIG. 3. The same as in Fig. 2 for the channel with nonequal partly diffuse boundaries described by $r_\varphi = \exp[-(\gamma^{-1} - 1) \sin^2 \varphi]$ with $\gamma = 1/3$ ($l_S/l \simeq 1.7$) at $y = 0$ and $\gamma = 2/3$ ($l_S/l \simeq 6.0$) at $y = L$. The inset shows the region near $y = L$ and additional plots (circles) for the model of angle-independent specularity parameter with $r = 0.49$ ($l_S/l \simeq 1.7$) at $y = 0$ and $r = 0.82$ ($l_S/l \simeq 6.0$) at $y = L$.

according to $l_e \simeq v \hbar \varepsilon_F / T^2$, the chosen ratios $l_1/L = 5$ and $l_1/l_e = 25$ can be achieved in GaAs 2D channels with $L \simeq 1.5 \mu\text{m}$ at the densities $n \simeq 5 \times 10^{11} \text{ cm}^{-2}$ and temperatures $T \simeq 40 \text{ K}$. For equal boundaries, typical profiles of $j(y)$ and $V(y)$ [26–28] are realized (Fig. 2), whereas the boundaries of different specularities lead to asymmetric profiles (Fig. 3). In both cases, the hydrodynamic approximation shows good agreement with the numerical solution at $B = 0$. For highly diffuse boundaries (Fig. 2), the agreement is improved by using the exact l_S . Within the narrow Knudsen layers near the boundaries, the difference between the hydrodynamic and kinetic solutions is maximal, and the kinetic solution becomes most sensitive to the choice of specularity parameter model (Fig. 3, inset). The sign of this difference correlates with the sign of δl_S . Good agreement is also found at finite B , although the slopes of $j(y)$ expectedly differ near the boundaries within the cyclotron diameter $2R_c$ which defines the effective Knudsen layer at $R_c < l$. A detailed discussion of the underlying physics requires a solution of the problem of exact slip length in the presence of a magnetic field, which is the subject for a future study.

To summarize, a direct link between the BC for the distribution function and Maxwell's BC for the drift velocity is given by the approximate expression of the boundary slip length l_S through the specularity parameter characterizing properties of the boundary scattering [Eqs. (10)–(12)]. For a gas of charged fermions in magnetic field B , l_S is B dependent and anisotropic, reflecting the behavior of the viscosity. The exact l_S , calculated at $B = 0$ for several models of angle-dependent specularity parameter, is within a few percent from the approximate one and converges to it with increasing specularity [Fig. 1]. This finding, together with applications of the results to Poiseuille flow [Figs. 2 and 3], proves that the approximate expression for l_S works much better than one might initially expect.

- [1] R. N. Gurzhi, Sov. Phys. JETP **17**, 521 (1963); *Sov. Phys. Usp.* **11**, 255 (1968).
- [2] M. J. M. de Jong and L. W. Molenkamp, *Phys. Rev. B* **51**, 13389 (1995).
- [3] M. Müller, J. Schmalian, and L. Fritz, *Phys. Rev. Lett.* **103**, 025301 (2009).
- [4] R. Bistritzer and A. H. MacDonald, *Phys. Rev. B* **80**, 085109 (2009).
- [5] A. V. Andreev, S. A. Kivelson, and B. Spivak, *Phys. Rev. Lett.* **106**, 256804 (2011).
- [6] B. N. Narozhny, I. V. Gornyi, M. Titov, M. Schütt, and A. D. Mirlin, *Phys. Rev. B* **91**, 035414 (2015).
- [7] I. Torre, A. Tomadin, A. K. Geim, and M. Polini, *Phys. Rev. B* **92**, 165433 (2015).
- [8] D. A. Bandurin, I. Torre, R. Krishna Kumar, M. Ben Shalom, A. Tomadin, A. Principi, G. H. Auton, E. Khestanova, K. S. Novoselov, I. V. Grigorieva, L. A. Ponomarenko, A. K. Geim, and M. Polini, *Science* **351**, 1055 (2016).
- [9] P. S. Alekseev, *Phys. Rev. Lett.* **117**, 166601 (2016).
- [10] A. Lucas, J. Crossno, K. C. Fong, P. Kim, and S. Sachdev, *Phys. Rev. B* **93**, 075426 (2016).
- [11] A. Principi, G. Vignale, M. Carrega, and M. Polini, *Phys. Rev. B* **93**, 125410 (2016).
- [12] F. M. D. Pellegrino, I. Torre, A. K. Geim, and M. Polini, *Phys. Rev. B* **94**, 155414 (2016).
- [13] T. Scaffidi, N. Nandi, B. Schmidt, A. P. Mackenzie, and J. E. Moore, *Phys. Rev. Lett.* **118**, 226601 (2017).
- [14] F. M. D. Pellegrino, I. Torre, and M. Polini, *Phys. Rev. B* **96**, 195401 (2017).
- [15] G. Falkovich and L. Levitov, *Phys. Rev. Lett.* **119**, 066601 (2017).
- [16] A. Levchenko, H.-Y. Xie, and A. V. Andreev, *Phys. Rev. B* **95**, 121301(R) (2017).
- [17] A. Lucas, *Phys. Rev. B* **95**, 115425 (2017).
- [18] D. A. Bandurin, A. V. Shytov, L. S. Levitov, R. Krishna Kumar, A. I. Berdyugin, M. Ben Shalom, I. V. Grigorieva, A. K. Geim, and G. Falkovich, *Nat. Commun.* **9**, 4533 (2018).
- [19] A. Lucas and S. A. Hartnoll, *Phys. Rev. B* **97**, 045105 (2018).
- [20] A. Lucas and K. C. Fong, *J. Phys.: Condens. Matter* **30**, 053001 (2018).
- [21] G. M. Gusev, A. D. Levin, E. V. Levinson, and A. K. Bakarov, *AIP Adv.* **8**, 025318 (2018).
- [22] G. M. Gusev, A. D. Levin, E. V. Levinson, and A. K. Bakarov, *Phys. Rev. B* **98**, 161303(R) (2018).
- [23] A. D. Levin, G. M. Gusev, E. V. Levinson, Z. D. Kvon, and A. K. Bakarov, *Phys. Rev. B* **97**, 245308 (2018).
- [24] P. S. Alekseev and M. A. Semina, *Phys. Rev. B* **98**, 165412 (2018).
- [25] M. Chandra, G. Kataria, D. Sahdev, and R. Sundararaman, *Phys. Rev. B* **99**, 165409 (2019).
- [26] J. A. Sulpizio, L. Ella, A. Rozen, J. Birkbeck, D. J. Perello, D. Dutta, M. Ben-Shalom, T. Taniguchi, K. Watanabe, T. Holder, R. Queiroz, A. Principi, A. Stern, T. Scaffidi, A. K. Geim, and S. Ilani, *Nature (London)* **576**, 75 (2019).
- [27] T. Holder, R. Queiroz, T. Scaffidi, N. Silberstein, A. Rozen, J. A. Sulpizio, L. Ella, S. Ilani, and A. Stern, *Phys. Rev. B* **100**, 245305 (2019).
- [28] O. E. Raichev, G. M. Gusev, A. D. Levin, and A. K. Bakarov, *Phys. Rev. B* **101**, 235314 (2020).
- [29] A. Gupta, J. J. Heremans, G. Kataria, M. Chandra, S. Fallahi, G. C. Gardner, and M. J. Manfra, *Phys. Rev. Lett.* **126**, 076803 (2021).
- [30] H. Grad, *Principles of the Kinetic Theory of Gases*, Handbuch der Physik Vol. XII (Springer, Berlin, 1958), p. 205.
- [31] J. C. Maxwell, *Scientific Papers* (Dover, New York, 1953), Vol. 2, p. 704.
- [32] D. Einzel and J. M. Parpia, *J. Low Temp. Phys.* **109**, 1 (1997).
- [33] H. H. Jensen, H. Smith, P. Wolffe, K. Nagai, and T. M. Bisgaard, *J. Low Temp. Phys.* **41**, 473 (1980).
- [34] E. I. Kiselev and J. Schmalian, *Phys. Rev. B* **99**, 035430 (2019).
- [35] S. B. Soffer, *J. Appl. Phys.* **38**, 1710 (1967).
- [36] L. A. Fal'kovskii, Sov. Phys. JETP **31**, 981 (1970); L. A. Falkovsky, *Adv. Phys.* **32**, 753 (1983).
- [37] V. I. Okulov and V. V. Ustinov, Sov. Phys. JETP **40**, 584 (1975).
- [38] F. T. Vasko and O. E. Raichev, *Quantum Kinetic Theory and Applications* (Springer, New York, 2005).
- [39] Y. Guo, *Arch. Ration. Mech. Anal.* **197**, 713 (2010).
- [40] P. Welander, *Ark. Fys.* **7**, 507 (1954).
- [41] D. R. Willis, *Phys. Fluids* **5**, 127 (1962).
- [42] S. Albertoni, C. Cercignani, and L. Gotusso, *Phys. Fluids* **6**, 993 (1963).
- [43] D. Einzel, H. H. Jensen, H. Smith, and P. Wolffe, *J. Low Temp. Phys.* **53**, 695 (1983).
- [44] A. V. Latyshev and A. A. Yushmanov, *Teor. Mat. Fiz.* **129**, 491 (2001).
- [45] X.-J. Gu, D. R. Emerson, and G.-H. Tang, *Phys. Rev. E* **81**, 016313 (2010).